Relevance of NAC-2, an Na^+-coupled citrate transporter, to life span, body size and fat content in *Caenorhabditis elegans*

You-Jun FEI*[1], Jin-Cai LIU*, Katsuhisa INOUE*, Lina ZHUANG*, Katsuya MIYAKE†, Seiji MIYAUCHI* and Vadivel GANAPATHY*

*Department of Biochemistry and Molecular Biology, Medical College of Georgia, Augusta, GA 30912, U.S.A., and †Institute of Molecular Medicine and Genetics, Medical College of Georgia, Augusta, GA 30912, U.S.A.

We have cloned and functionally characterized an Na^+-coupled citrate transporter from *Caenorhabditis elegans* (ceNAC-2). This transporter shows significant sequence homology to *Drosophila* Indy and the mammalian Na^+-coupled citrate transporter NaCT (now known as NaC2). When heterologously expressed in a mammalian cell line or in *Xenopus* oocytes, the cloned ceNAC-2 mediates the Na^+-coupled transport of various intermediates of the citric acid cycle. However, it transports the tricarboxylate citrate more efficiently than dicarboxylates such as succinate, a feature different from that of ceNAC-1 (formerly known as ceNaDC1) and ceNAC-3 (formerly known as ceNaDC2). The transport process is electrogenic, as evidenced from the substrate-induced inward currents in oocytes expressing the transporter under voltage-clamp conditions. Expression studies using a reporter-gene fusion method in transgenic *C. elegans* show that the gene is expressed in the intestinal tract, the organ responsible for not only the digestion and absorption of nutrients but also for the storage of energy in this organism. Functional knockdown of the transporter by RNAi (RNA interference) not only leads to a significant increase in life span, but also causes a significant decrease in body size and fat content. The substrates of ceNAC-2 play a critical role in metabolic energy production and in the biosynthesis of cholesterol and fatty acids. The present studies suggest that the knockdown of these metabolic functions by RNAi is linked to an extension of life span and a decrease in fat content and body size.

Key words: body size, *Caenorhabditis elegans*, fat synthesis, life span, RNA interference (RNAi), sodium-coupled citrate transporter.

INTRODUCTION

Recently we have cloned and functionally characterized two Na^+-coupled dicarboxylate transporters from *Caenorhabditis elegans*, namely ceNAC-1 (formerly known as ceNaDC1) and ceNAC-3 (formerly known as ceNaDC2) [1]. These two transporters show significant sequence homology to the Na^+-coupled dicarboxylate carriers/transporters (NaDCs) identified in mammals and in *Xenopus laevis* (NaDC1, NaDC2 and NaDC3) [2]. Functional studies using a mammalian heterologous expression system have shown that the cloned ceNAC-1 and ceNAC-3 mediate Na^+-coupled transport of various dicarboxylates. With succinate as the substrate, ceNAC-1 exhibits much lower affinity compared with ceNAC-3. Therefore, ceNAC-1 and ceNAC-3 correspond at the functional level to mammalian NaDC1 and NaDC3, respectively [3–12]. Individual functional inactivation of these two transporter genes in *C. elegans* by RNAi (RNA interference) suggests that ceNAC-1 is not relevant to the regulation of life span in this organism, whereas the knockdown of ceNAC-3 leads to a significant extension of the mean and maximum life span [1]. In this respect, ceNAC-3 is similar to the di- and tricarboxylate transporter Indy identified recently in *Drosophila melanogaster* (drIndy) [13–15]. The *indy* gene, when in a p-element mutant heterozygote, confers longevity in *Drosophila*, possibly because disruption of the function of the *indy* gene may lead to decreased availability of di- and tricarboxylates for cellular production of metabolic energy. Thus the disruption of this transporter function may create a biological state similar to that of caloric restriction, and consequently lead to life-span extension.

However, drIndy is a cation-independent and electroneutral transporter for a variety of TCA (tricarboxylic acid) cycle intermediates, with preference for the tricarboxylate citrate compared with dicarboxylates such as succinate [14,15]. These characteristics of drIndy differ from those of ceNAC-3, indicating that ceNAC-3 may not be the *C. elegans* counterpart of drIndy, even though both genes are associated with the regulation of the life span of the respective organisms. Since ceNAC-3 is the orthologue of the mammalian NaDC3, this also rules out NaDC3 as the mammalian counterpart of drIndy. In our search for mammalian Indy, we were able to identify a third member of the NaDC family in mammals, which transports citrate very efficiently [16–18]. We designated this transporter NaCT (Na^+-coupled citrate transporter) to indicate its ability to recognize citrate as the preferential substrate. Mammalian NaCT (now known as NaC2), expressed primarily in the liver, is involved in the utilization of extracellular citrate for the hepatic synthesis of fat [18]. Even though the mammalian NaCT is similar to drIndy with respect to the recognition of citrate as a substrate, NaCT differs from drIndy in terms of Na^+-dependence. Therefore, it is not known at this time whether or not NaCT is the functional counterpart of drIndy. It is also not known whether NaCT plays any role as a determinant of life span in mammals, as does drIndy in *Drosophila*. To evaluate the potential role of NaCT in life-span regulation, we asked whether there is an orthologue of NaCT in *C. elegans* and, if there is,

Abbreviations used: NaDC, Na^+-coupled dicarboxylate carrier/transporter; ceNAC-2, *Caenorhabditis elegans* Na^+-coupled citrate transporter; drIndy, *Drosophila* Indy; NaCT, Na^+-coupled citrate transporter; GFP, green fluorescent protein; HRPE, human retinal pigment epithelial; dsRNA, double-stranded RNA; cRNA, complementary RNA; RNAi, RNA interference; TCA, tricarboxylic acid; TEVC, two-electrode voltage-clamp.

[1] To whom correspondence should be addressed (e-mail yjfei@mail.mcg.edu).

The ceNAC-2 cDNA and its encoded transporter protein sequences have been deposited in the GenBank Nucleotide Sequence Database under accession number AY090486.

whether the transporter plays a role as a determinant of life span in the organism. In this report we describe the functional aspects of the cloned ceNAC-2 (*C. elegans* Na^+-coupled citrate transporter; the orthologue of mammalian NaCT/NaC2) and their relevance to animal life span, body size and fat content.

MATERIALS AND METHODS

Materials

[^{14}C]Citrate and [^{3}H]succinate were purchased from Moravek Biochemicals (Brea, CA, U.S.A.). The human retinal pigment epithelial (HRPE) cell line was maintained in Dulbecco's minimum essential medium/F-12 medium supplemented with 10 % fetal bovine serum, 100 units/ml penicillin and 100 μg/ml streptomycin. Lipofectin was purchased from Invitrogen (Carlsbad, CA, U.S.A.). Restriction enzymes were obtained from New England Biolabs (Beverly, MA, U.S.A.). Unlabelled monocarboxylates, dicarboxylates and tricarboxylates were obtained from Sigma (St. Louis, MO, U.S.A.).

Nematode culture and RNA preparation

A wild-type nematode strain, *C. elegans* N2 (Bristol), was obtained from the *Caenorhabditis* Genetics Center (St. Paul, MN, U.S.A.). Nematode culture was carried out using a standard procedure with a large-scale liquid cultivation protocol [1,19–22]. The nematodes were cleaned by sedimentation through 15 % (w/v) Ficoll 400 in 0.1 M NaCl. The pellet was then used for total RNA preparation. Total RNA was isolated using the TRIzol reagent (Gibco-BRL, Gaithersburg, MD, U.S.A.). Poly(A)$^+$ mRNA was purified by affinity chromatography using oligo(dT)-cellulose.

Cloning of *C. elegans* NAC-2

A search of the WormBase with mammalian NaCT/NaC2 as the query identified a putative gene in cosmid R107.1 (GenBank accession no. Z14092) that most probably codes for the *C. elegans* orthologue of NaCT/NaC2. A pair of PCR primers specific for this gene was designed: forward primer, 5′-CTC CAT CGA AGA ATC GCA C-3′; and reverse primer, 5′-GAA ATA GCA TAC CCA GCA CC-3′. These primers yielded a single reverse transcriptase PCR product ($\approx$ 1.0 kb) with RNA from *C. elegans*. The reverse transcriptase PCR product was subcloned into pGEM-T easy vector (Promega, Madison, WI, U.S.A.). The molecular identity of the insert was established by sequencing. This cDNA fragment was used as a probe to screen a *C. elegans* cDNA library to isolate the full-length clone. SuperScript Plasmid System from Gibco-BRL was used to establish the cDNA library using the poly(A)$^+$ RNA from *C. elegans* as described in [21,22].

Vaccinia/T7 expression system

Functional expression of the ceNAC-2 cDNA in HRPE cells was done using the vaccinia virus expression system. Uptake of [^{14}C]citrate and [^{3}H]succinate was determined at 37 °C as described previously [1,16–18]. In most experiments, the uptake medium was 25 mM Hepes/Tris (pH 7.5), containing 140 mM NaCl, 5.4 mM KCl, 1.8 mM $CaCl_2$, 0.8 mM $MgSO_4$ and 5 mM glucose. Experiments were performed in duplicate and each experiment was repeated three times. Results are presented as means $\pm$ S.E.M.

Electrophysiological studies of ceNAC-2 transport function

The coding sequence of ceNAC-2 cDNA was amplified by PCR using the following primers: 5′-CCC GGG TAT GAA GCC TAG CCC CCA GCG TAC GTT AAT AAA A-3′ (forward primer) and 5′-GCG GAT CCA AAA ATT AGC AAA CTG GAT ATG AAG AGT TTT CTG AAG-3′ (reverse primer). The PCR-derived ceNAC-2 coding fragment was then inserted into the *Xma*I/*Bam*HI site in the oocyte expression vector pGH19 (a generous gift from Dr Peter S. Aronson, Yale University, School of Medicine, New Haven, CT, U.S.A.). In this construct, the ceNAC-2 coding sequence was flanked by regulatory elements in the 5′- and 3′-untranslated regions of the *Xenopus* β-globin gene. Plasmid pGH19-ceNaCT cDNA was linearized with *Xho*I and transcribed *in vitro* using the mMESSAGE mMACHINE RNA transcription kit (Ambion, Austin, TX, U.S.A.). The cRNA (complementary RNA) was injected into the *Xenopus* oocytes. The procedures for oocyte uptake and electrophysiological studies using the TEVC (two-electrode voltage-clamp) protocol have been described previously [21–24].

Analysis of tissue expression pattern of ceNAC-2

This was done by the analysis of GFP (green fluorescent protein) expression in transgenic *C. elegans* that were engineered to express a transcriptional *nac-2*::*gfp* fusion construct. The cosmid R107 containing the *C. elegans nac-2* gene and its promoter was obtained from the Sanger Center (Hinxton, Cambridge, U.K.). A DNA fragment ($\approx$ 2.1 kb) containing the *C. elegans nac-2* gene promoter region was generated by PCR using this cosmid DNA as the template. The sense primer (co-ordinates in cosmid R107 are 11 660–11 630) with a *Sal*I adapter attached to the 5′-end was 5′-GTC GAC GAG GTG TTA AAC TGT ATA GTC GTG GTG-3′ and the reverse primer (co-ordinates in cosmid R107 are 9609–9637) with a *Bam*HI adapter attached to the 5′-end was 5′-GCC GGA TCC AAG AAG TAC CAG AAG CTT TTT TAT-3′. This promoter element was then inserted into the GFP-expression vector pPD117.01 (kindly provided by Dr A. Fire, Carnegie Institution of Washington, Baltimore, MD, U.S.A.) at a *Sal*I/*Bam*HI site upstream of the GFP coding sequence. Transgenic lines expressing this fusion construct were established using a standard germ-line-transformation protocol [25,26]. GFP expression pattern was determined by fluorescence microscopy [26–28].

Life-span and body-size measurements under the influence of *nac-2*-gene-specific RNAi

A fragment of the coding region of ceNAC-2 cDNA was generated by PCR and subcloned into a 'double T7' plasmid pPD129.36, which was subsequently transformed into *Escherichia coli* HT115 (DE3) cells [29,30]. Induction of HT115 cells harbouring the double-T7 plasmid to express dsRNA (double-stranded RNA), the bacterium-mediated RNAi procedure and life-span measurement of age-synchronous nematodes were carried out as described previously [1]. Mean life spans from different groups were compared using the non-parametric log-rank analysis. The survival curves were plotted according to the Kaplan–Meier algorithm using Minitab software (version 13; Minitab, State College, PA, U.S.A.). Nematode body-size measurement was made on day 5. Worms were placed on agar plates and anaesthetized using 0.1 M NaN_3. To facilitate measurement, worms were laid out straight using a platinum wire. Measurement was carried out under a dissecting microscope, with an eyepiece graticule calibrated with a stage micrometer (Olympus, Melville, NY, U.S.A.). To calculate body volume, worms were treated as cylinders: $V = \pi(1/2D)^2L$, where D is the body width and L is body length [31].

Fat-content analysis by laser-scanning confocal microscopy

Fat storage droplets in living *C. elegans* were visualized using the vital dye Nile Red (Molecular Probes, Eugene, OR, U.S.A.). Eggs,

obtained from gravid hermaphrodites using an alkaline hypochlorite treatment procedure, were dispensed on NGM Petri dishes with bacterial lawns and allowed to hatch. The isopropyl β-D-thiogalactoside-induced HT115 bacterial suspension harbouring *cenac-2*-gene-specific dsRNA was mixed with an equal volume of Nile Red solution (0.1 μg/ml) and fed to the newly hatched worms on individual Petri dishes every day until the worms developed into adults [1,32,33]. Nile Red-stained worms were examined by a Zeiss Axioplan-2 microscope (Carl Zeiss MicroImaging, Thornwood, NY, U.S.A.). All Nile Red images were acquired using identical settings and exposure times. The excitation filter wavelength was 515–560 nm and the emission filter wavelength was >590 nm. Fluorescence intensity was quantified using the LSM 510 software (Carl-Zeiss, Heidelberg, Germany).

RESULTS

Molecular cloning and structural characterization of ceNAC-2

The *C. elegans nac-2* gene is localized on chromosome III and its size is at least ≈ 2.7 kb, excluding the promoter region. The gene consists of 11 exons as deduced by a comparison between the sequence of the cloned cDNA with that of the GenBank deposit R107.1 from the nematode genome sequence project (WormBase release WS93). The ceNAC-2 cDNA is 1747 bp long and contains a poly(A)$^+$ tail. The 5′- and 3′-untranslated regions are 30 and 44 bp long, respectively. The ceNAC-2 protein deduced from the cDNA sequence contains 551 amino acids with an estimated molecular mass of 61 kDa. The ceNAC-2 cDNA and its encoded transporter protein sequences have been deposited in GenBank (accession number AY090486). A pairwise comparison analysis of the transporter protein sequences between ceNAC-2 and its closely related functional counterparts, the mammalian NaCT/NaC2 and drIndy, using the BESTFIT algorithm in the GCG package (version 10.2; Madison, WI, U.S.A.) has shown that ceNAC-2 is closely related to mammalian NaCT/NaC2 (49 % similarity and 36 % identity) and to drIndy (48 % similarity and 35 % identity). ceNAC-2 also exhibits close homology to the other two Na$^+$-carboxylate transporters identified in *C. elegans*, namely NaDC1/NAC-1 and NaDC2/NAC-3 (49 and 47 % sequence similarity, respectively).

Functional characterization of ceNAC-2 using a heterologous mammalian expression system

The functional analysis of the cloned ceNAC-2 was carried out by heterologous expression of the cDNA in HRPE cells using the vaccinia virus expression system. The uptake of [^{14}C]citrate (10 μM) in the presence of extracellular Na$^+$ (pH 7.5) increased $\approx$45-fold in cells expressing ceNAC-2 (61 ± 5 pmol/10^6 cells per min) compared with vector-transfected control cells (1.3 ± 0.1 pmol/10^6 cells per min; results not shown). The uptake of succinate was also increased markedly in ceNAC-2-expressing cells compared with control cells. However, the ability of ceNAC-2 to transport citrate was much greater than its ability to transport succinate, when measured under identical conditions (10 μM substrate). Since we have already shown that succinate is a substrate for the previously cloned ceNAC-1 and ceNAC-3, we compared the abilities of all three transporters to transport citrate and succinate under identical conditions. As shown previously, ceNAC-1 and ceNAC-3 were able to transport succinate very effectively (Figure 1A). The magnitude of succinate transport was comparable between ceNAC-3 and ceNAC-2, whereas that of ceNAC-1 was a little lower. In contrast, the magnitude of citrate transport was the highest for ceNAC-2. ceNAC-3 showed only a minimal ability to transport this tricarboxylate. The ability of ceNAC-1 to transport citrate was much higher than that of ceNAC-3 but much lower than that of ceNAC-2. These data show that, among these three transporters, ceNAC-2 is the only transporter that has citrate as its preferred substrate. The ceNAC-2-mediated citrate uptake was obligatorily dependent on the presence of Na$^+$ because substitution of Na$^+$ with Li$^+$, K$^+$ or *N*-methyl-D-glucamine abolished completely the cDNA-induced increase in citrate uptake. There was no involvement of chloride in the uptake process, as indicated by comparable uptake activities in the presence of NaCl or sodium gluconate (results not shown).

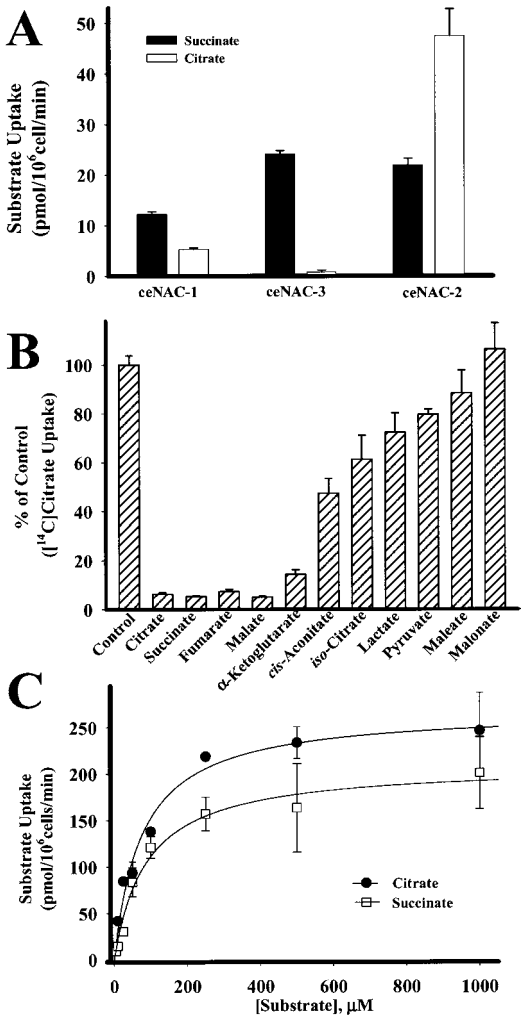

Figure 1 Functional characteristics of *C. elegans* NAC-2 in a mammalian cell expression system

(**A**) Comparison of the transport activities of NAC-1, NAC-3 and NAC-2 from *C. elegans*. Uptake of 10 μM citrate or 10 μM succinate was measured in HRPE cells transfected with the transporter cDNAs. Values (cDNA-specific activity) represent means $\pm$ S.E.M. from six determinations. (**B**) Substrate specificity of ceNAC-2-mediated uptake. Uptake of 15 μM [^{14}C]citrate was measured in the absence or presence of potential inhibitors (2.5 mM) in cells transfected with vector alone or ceNAC-2 cDNA. The cDNA-specific uptake in the absence of inhibitors was taken as the control (100 %) and the uptake in the presence of inhibitors is given as a percentage of this control value. (**C**) Saturation kinetics of citrate and succinate uptake mediated by ceNAC-2 in HRPE cells. Uptake of citrate or succinate was measured in a NaCl-containing medium (pH 7.5) over a substrate concentration range of 10–1000 μM in cells transfected with ceNAC-2 cDNA. Values (cDNA-specific activity) represent means $\pm$ S.E.M. from six determinations.

The substrate specificity of ceNAC-2 was studied by monitoring the ability of various monocarboxylates, dicarboxylates and tricarboxylates (2.5 mM) to compete with [^{14}C]citrate (15 μM) for

the uptake process. Uptake measurements were made in parallel in vector-transfected cells and in cDNA-transfected cells and the cDNA-specific uptake was calculated by subtracting the uptake in vector-transfected cells from the uptake in cDNA-transfected cells. Only the cDNA-specific uptake was used in the analysis. Unlabelled citrate was a potent inhibitor of [^{14}C]citrate uptake (Figure 1B). Interestingly, the two other tricarboxylates that we tested, namely isocitrate and *cis*-aconitate, did not compete with [^{14}C]citrate as effectively as unlabelled citrate. Among the various dicarboxylates tested, the ceNaC-2-mediated citrate uptake was inhibited markedly by succinate, α-ketoglutarate, fumarate and malate. In contrast to fumarate, its stereoisomer maleate failed to compete with citrate. Similarly, malonate, a structural homologue of succinate, also failed to inhibit the uptake of citrate. The monocarboxylates pyruvate and lactate caused only minimal inhibition.

The transport of citrate via ceNAC-2 was saturable with a Michaelis–Menten constant (K_t) of 76 ± 14 μM at pH 7.5 (Figure 1C). The corresponding value for succinate was 88 ± 13 μM under identical conditions. These data show that ceNAC-2 is a high-affinity Na^+-coupled transporter for the tricarboxylate citrate and the dicarboxylate succinate. Interestingly, even though the affinities for citrate and succinate are comparable, the transport rate for citrate is much greater than for succinate, suggesting that the transport processes of these two substrates differ in their maximal velocity (V_{max}). This is evident from the V_{max} values for these two substrates (270 ± 13 pmol/10^6 cells per min for citrate versus 210 ± 8 pmol/10^6 cells per min for succinate). These characteristics are different from those of ceNAC-1 and ceNAC-3. Thus the transport features of ceNAC-2 are similar to those of drIndy. However, ceNAC-2 and drIndy differ in their dependence on Na^+. ceNAC-2 is also similar to the recently identified mammalian NaCT/NaC2 not only in Na^+-dependence but also in the ability to transport citrate much more effectively than succinate.

Functional characterization of ceNAC-2 using the *X. laevis* oocyte expression system

To determine whether the transport process of ceNAC-2 is electrogenic, we used the *X. laevis* oocyte expression system to express ceNAC-2 heterologously. First, we tested whether the transporter is expressed in oocytes injected with ceNAC-2 cRNA by measuring the uptake of [^{14}C]citrate (40 μM). The uptake in cRNA-injected oocytes was 12.9 ± 0.8 pmol/oocyte per 15 min. This value was about 45-fold higher than the uptake measured under identical conditions in oocytes injected with water (0.3 ± 0.01 pmol/oocyte per 15 min; Figure 2A). Next, we examined the electrogenic nature of the transport process. Perifusion of the ceNAC-2 cRNA-injected oocytes with citrate (250 μM) in the presence of Na^+ (100 mM NaCl) induced inward currents, detectable by the TEVC method at a holding membrane potential of -50 mV (Figure 2B). Perifusion of the oocytes with succinate also induced similar inward currents, although the magnitude of the currents was less than that induced by citrate (results not shown). These data show unequivocally that the ceNAC-2-mediated transport process is electrogenic irrespective of whether the transported substrate is a dicarboxylate or a tricarboxylate. The citrate- and succinate-induced currents were obligatorily dependent on the presence of Na^+. In the absence of Na^+ (NaCl was substituted by choline chloride), perifusion of the oocytes with citrate did not induce any detectable current (Figure 2B). On the other hand, when chloride in the perifusion buffer was replaced with gluconate, the citrate-induced current remained unaltered. These data show that the transport process mediated by ceNAC-2 is Na^+-dependent and that Cl^- ions do not have any role in the transport process.

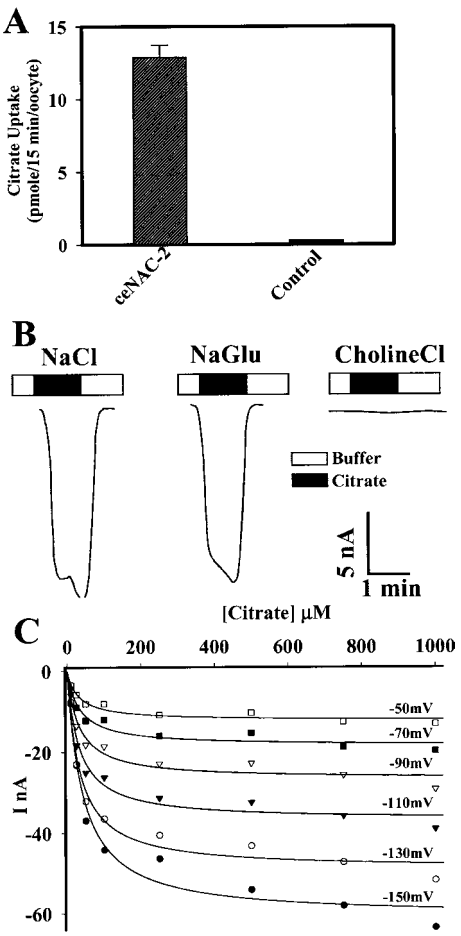

Figure 2 Functional characteristics of *C. elegans* NAC-2 in *Xenopus* oocyte expression system

(**A**) Uptake of [^{14}C]citrate (40 μM) was measured in control (water-injected) oocytes and in oocytes injected with ceNAC-2 cRNA in the presence of NaCl. Values represent means $\pm$ S.E.M. ($n = 8$–10 oocytes). (**B**) Ion-dependence of the citrate-evoked currents under voltage-clamp conditions in oocytes expressing ceNAC-2. Oocytes were sequentially superfused with 250 μM of citrate in the presence of iso-osmolar concentrations (100 mM) of NaCl, sodium gluconate (NaGlu) or choline chloride. (**C**) Kinetic analyses of citrate-evoked inward currents in oocytes expressing ceNAC-2 at different testing membrane potentials. The perifusion buffer contained NaCl.

The citrate-induced currents of ceNAC-2 were further analysed in terms of their dependence on membrane potential. Steady-state currents induced by citrate over a concentration range of 10 μM–1 mM were measured at different testing membrane potentials (-50 to -150 mV). At each of these testing membrane potentials, the citrate-induced currents were saturable with respect to citrate concentration (Figure 2C). The maximal current induced by citrate however increased with increasing testing membrane potential. The data show that the transport rate increases with increasing membrane potential, suggesting a role for membrane potential as a driving force for the transport process. Thus the transport process mediated by ceNAC-2 derives its driving force from the electrochemical Na^+ gradient. The relationship between the substrate concentration and the induced current was hyperbolic at each of the testing membrane potentials. We analysed the data at each of the testing membrane potentials according to the Michaelis–Menten equation. The Michaelis–Menten constant ($K_{0.5}$), the concentration of citrate needed for the induction of half-maximal current, was 34 ± 8 μM at a testing membrane potential of -70 mV. This value did not change significantly with different

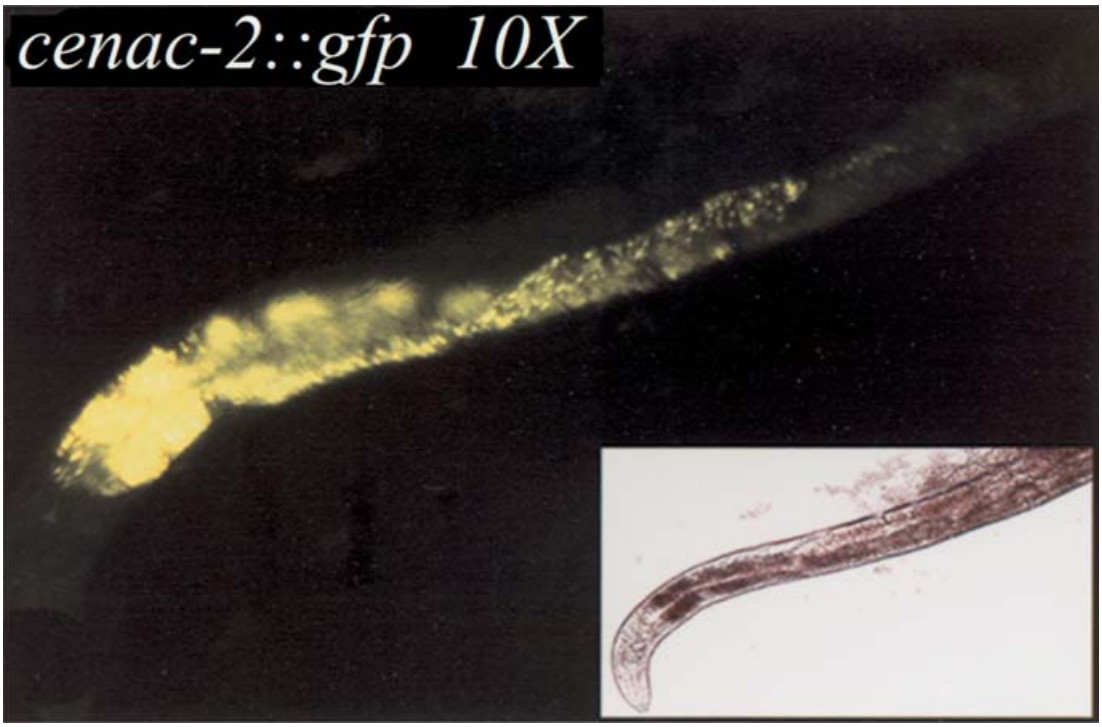

Figure 3 Tissue expression pattern of *nac-2* gene in *C. elegans*

Expression of GFP was driven by the *nac-2* gene promoter in the transformed transgenic *C. elegans*. A GFP image of a representative young adult worm is shown and the inset is the bright-field image.

testing membrane potentials. However, the maximal current (I_{max}) increased with increasing testing membrane potential. The value for I_{max} was 12.3 ± 0.6 nA at a testing membrane potential of -50 mV and this value increased gradually to 61.1 ± 2.6 nA as the testing membrane potential increased to -150 mV. These data show that the membrane potential does not influence the substrate affinity of the transporter but it enhances the maximal velocity of the transport process.

Tissue expression pattern of the *nac-2* gene

We investigated the tissue expression pattern of the *nac-2* gene in *C. elegans* using the transgenic GFP fusion technique in which the transgene consisted of the *nac-2*-gene-specific promoter fused with GFP cDNA. The expression of GFP in this fusion gene is controlled by the *nac-2*-gene-specific promoter. Therefore, the expression pattern of GFP in transgenic *C. elegans* expressing the fusion gene is likely to match the expression pattern of the native *nac-2* gene. With this technique, we found that GFP expression is restricted to the intestinal tract in this organism (Figure 3). This expression pattern is evident from the early larva stage through the adult stage (results not shown). The GFP fluorescence is detectable throughout the intestinal tract, starting from the pharynx all the way through the anus. The expression level of GFP is significantly greater in the anterior half of the intestine than in the posterior half. This expression pattern was confirmed with at least 10 transgenic animals.

Influence of RNAi-mediated knockdown of *nac-2* on life span, body size and fat deposit

Knockdown of *nac-2* by feeding wild-type N2 worms with bacteria expressing the *cenac-2*-specific dsRNA caused a significant increase in both average and maximal life span of the organism (Figure 4A). The mean life span of the worms fed on bacteria harbouring *cenac-2*-specific dsRNA was 19.4 ± 0.3 days ($n = 211$); mean life span of the worms fed on bacteria harbouring the empty vector pPD129 was the same as that of wild-type N2 worms (16.3 ± 0.2 days; $n = 180$). The increase in average life span induced by *cenac-2* knockdown was 19% ($P < 0.001$). A *daf-2* knockdown was included as a positive control in these experiments. Worms fed on bacteria expressing *daf-2*-specific dsRNA exhibited an average life span of 31.4 ± 0.6 days ($n = 60$), showing that knockdown of *daf-2* doubles the average life span. This influence of *daf-2* knockdown on life span is similar to that observed with conditional partial loss of the function of the *daf-2* gene [34,35]. In addition, a 'lean' phenotype was detected when the *nac-2* gene was knocked down by bacteria-mediated RNAi approach. Body length and body width were smaller in *nac-2*-RNAi worms than in control worms. The calculated body size was significantly reduced ($\approx 40\%$; $P < 0.001$) in *nac-2*-RNAi worms (2.95 ± 0.13 nl, $n = 60$) in comparison with the control vector-fed worms (4.91 ± 0.05 nl, $n = 58$; Figure 4B). This interesting phenotype was not observed when ceNAC-1 or ceNAC-3 was knocked down by a similar experimental approach (*nac-1* knockdown, 4.92 ± 0.07 nl, $n = 45$; *nac-3* knockdown, 5.05 ± 0.07 nl, $n = 53$).

The intestinal fat content was also analysed by laser confocal fluorescence microscopy approach using Nile Red (5H-benzo [α]phenoxazine-5-one, 9-diethylamino) to stain intracellular lipid droplets in live *C. elegans* under the influence of the *cenac-2* gene-specific RNAi. The intensity of Nile Red staining in this organism was reduced markedly ($56 \pm 6\%$ of the control value) when the *nac-2* was knocked down by RNAi ($P < 0.001$, $n = 13$; Figure 5). In these experiments, the control worms ($n = 8$) were fed on bacteria harbouring empty vector pPD129.

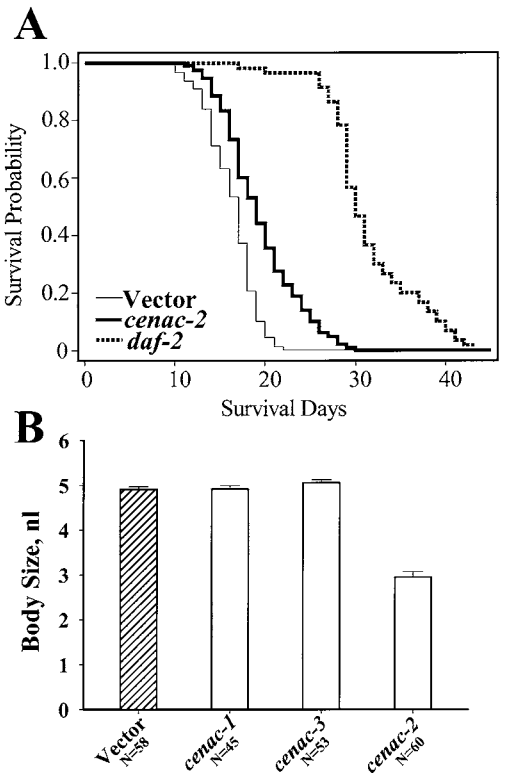

Figure 4 Effect of *nac-2* knockdown by RNAi on (A) life span and (B) body size in *C. elegans*

(**A**) The knockdown of *nac-2* was done by feeding the worms with bacteria producing *nac-2*-specific dsRNA. The knockdown of *daf-2* was included as a positive control. Worms fed on bacteria carrying the empty vector pPD129 served as the wild-type control. The curves show the survival probability of the worms in different experimental groups after hatching under the influence of the gene-specific dsRNAs. (**B**) Effect of the knockdown of *nac-2* by RNAi on body size in *C. elegans*. Data for the effects of the RNAi-mediated knockdown of *nac-1* and *nac-3* on the body size are included for comparison.

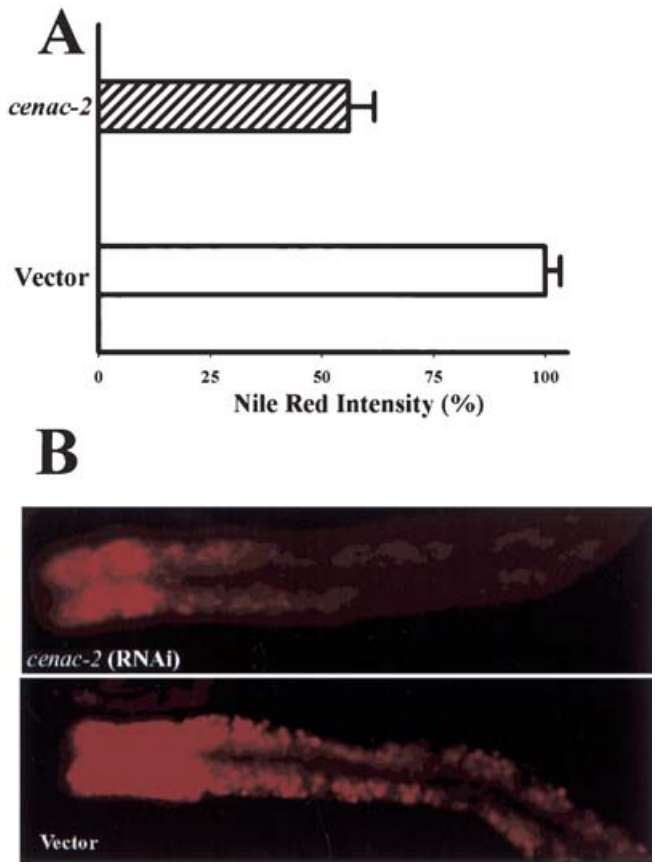

Figure 5 Effect of *nac-2* knockdown on fat deposition in *C. elegans*

(**A**) Comparison of the fluorescence intensity of Nile Red staining between worms with *nac-2* knockdown by RNAi (hatched bar; $n = 13$) and control worms (vector, empty bar; $n = 8$). The average intensity in control worms was taken as 100 %. (**B**) Representative fluorescence images of Nile Red staining in a worm with *nac-2* knockdown and in a control worm.

DISCUSSION

We have described in this paper the cloning and functional characterization of a Na^+-coupled citrate transporter (ceNAC-2) in *C. elegans*. This transporter is structurally similar to the previously cloned NAC-1 and NAC-3 in this organism [1]. The *C. elegans* NAC-2 transports the tricarboxylate citrate as well as several dicarboxylates such as succinate and α-ketoglutarate. The transport process is Na^+-dependent, Cl^--independent and electrogenic for both substrates. Functionally, the *C. elegans* NAC-2 is similar to the recently identified mammalian NaCT/NaC2 [16–18]. The *C. elegans* NAC-2 and the mammalian NaCT/NaC2 are structurally similar to drIndy [13–15]. NaCTs/NaC2s are also similar to drIndy with respect to their ability to recognize citrate as a substrate. However, drIndy is an Na^+-independent citrate transporter. The transport characteristics of *C. elegans* NAC-2 are distinct from those of NAC-1 and NAC-3 previously identified in this organism. The NAC-1 and NAC-3 transport succinate and other dicarboxylates much more effectively than citrate. Thus, NAC-1 and NAC-3 in *C. elegans* correspond to mammalian NaDC1/NaC1 and NaDC3/NaC3, whereas the transporter reported in this paper corresponds to mammalian NaCT/NaC2.

The unique functional feature of *C. elegans* NAC-2 is its ability to transport the tricarboxylate citrate as well as dicarboxylates such as succinate. Mammalian NaDCs (NaDC1/NaC1 and NaDC3/NaC3) are able to transport only dicarboxylates. Even though these transporters can transport citrate, it is only the dianionic form of citrate that is recognized as the substrate. Therefore, mammalian NaDC1/NaC1 and NaDC3/NaC3 are truly Na^+-coupled dicarboxylate transporters. We hypothesize that the NAC-1 and NAC-3 expressed in *C. elegans* also behave in a similar manner with respect to interaction with their substrates. In contrast, mammalian NaCTs/NaC2s and ceNAC-2 appear to possess the ability to transport dicarboxylates as well as the tricarboxylate citrate.

We also provide here information on the electrophysiological characteristics of *C. elegans* NAC-2. The transport process involves transfer of positive charge across the membrane irrespective of whether the transported substrate is a tricarboxylate or a dicarboxylate. Since the transport of citrate, a tricarboxylate, is an electrogenic process, there should be at least four Na^+ ions involved in the transport process. The predicted Na^+/substrate stoichiometry of 4:1 makes NAC-2 a very efficient concentrative transporter. In addition to the chemical Na^+ gradient, the membrane potential also serves as a driving force for this transporter. However, the substrate affinity of the transporter is not influenced by membrane potential, but the maximal velocity of the transport process is enhanced markedly by hyperpolarization.

Irrespective of the charge of the transported substrate, the transport process mediated by *C. elegans* NAC-2 is electrogenic. This

predicts that at least four Na^+ ions are involved in the transport process. If the Na^+/substrate stoichiometry is 4:1 irrespective of the charge nature of the substrate, the net transfer of charge across the membrane is expected to differ depending on whether the transported substrate is a tricarboxylate or a dicarboxylate. The transport of citrate, a tricarboxylate, would result in the transfer of only one positive charge whereas the transport of dicarboxylates such as succinate would result in the transfer of two positive charges. The amount of charge that is transferred across the membrane during the transport process can be quantified electrophysiologically in *X. laevis* oocytes by measuring the charge transfer and the substrate transfer simultaneously. Unfortunately, we could not perform these studies in the case of *C. elegans* NAC-2 because the magnitude of the currents induced by the transport process was not high enough for such measurements.

Since citrate is an excellent substrate for NAC-2, we hypothesized that the physiological function of this transporter is to facilitate the utilization of extracellular citrate and other TCA cycle intermediates for energy production. The successful cloning of this transporter from *C. elegans* has provided an opportunity to test this hypothesis. If caloric restriction leads to life-span extension, disruption of the function of NAC-2 is expected to enhance the life span. Studies of *nac-2* knockdown using the RNAi technique in *C. elegans* showed that this indeed was the case. Suppression of NAC-2 function does lead to a significant increase in average life span of the organism. Interestingly, our previous studies have shown that suppression of NAC-3 function also leads to life-span extension. This is not surprising because both NAC-2 and NAC-3 are functionally similar in terms of transport of succinate and other dicarboxylate intermediates of TCA cycle. Therefore, knockdown of *nac-2* or *nac-3* is expected to impair the utilization of succinate and other TCA cycle intermediates for energy production. This would create a metabolic state similar to that of caloric restriction and hence lead to life-span extension. However, even though NAC-2 and NAC-3 are similar in their ability to transport succinate and other dicarboxylates, they differ markedly in their ability to transport citrate. This tricarboxylate occupies a unique position in metabolism in that it is not only an intermediate in the TCA cycle but also a precursor for the biosynthesis of fatty acids, cholesterol and isoprenoids. We have demonstrated in the present study that the knockdown of *nac-2* leads to a significant decrease ($\approx$40%) in body size and a significant reduction (44%) in the fat content of the organism.

It is interesting to note that the knockdown of *nac-3* leads to an extension of life span without affecting the body size, whereas the knockdown of *nac-2* leads not only to life span extension but also to a decrease in body size and fat content. NAC-3 mediates the transport of dicarboxylates such as succinate and has no or little ability to transport citrate. In contrast, NAC-2 is able to transport citrate as well as dicarboxylates very effectively. Succinate and other dicarboxylate intermediates of the TCA cycle are capable of generating energy within the mitochondria. These metabolites can also be converted into citrate in the TCA cycle which then can exit the mitochondria to serve as a precursor for the synthesis of fatty acids and cholesterol in the cytoplasm. In contrast, citrate can directly enter the biosynthetic process for the generation of fatty acids and cholesterol in the cytoplasm. Furthermore, the plasma concentrations of citrate are much higher than those of the dicarboxylate intermediates of the TCA cycle in humans [36,37]. There is no information in the literature on the extracellular concentrations of citrate and other intermediates of the TCA cycle in *C. elegans*. If the extracellular concentrations of citrate are higher than those of succinate and other dicarboxylates in this organism as it is in humans, it is likely that the contribution of NAC-2 to the utilization of extracellular citrate and other TCA cycle intermediates for the generation of metabolic energy and for the synthesis of fatty acids and cholesterol is much greater than that of NAC-3. This might explain the differences in the biochemical consequences of *nac-2* knockdown and *nac-3* knockdown in *C. elegans*.

This work was supported by National Institutes of Health grants HD44404, HL64196 and AI49849 (V. G.) and by an intramural grant from the Medical College of Georgia Research Institute (Y.-J. F.).

REFERENCES

1 Fei, Y. J., Inoue, K. and Ganapathy, V. (2003) Structural and functional characteristics of two sodium-coupled dicarboxylate transporters (ceNaDC1 and ceNaDC2) from *Caenorhabditis elegans* and their relevance to life span. J. Biol. Chem. **278**, 6136–6144

2 Markovich, D. and Murer, H. (2004) The SLC13 gene family of sodium sulphate/carboxylate cotransporters. Pflugers Arch. Eur. J. Physiol., in the press

3 Pajor, A. M. (1995) Sequence and functional characterization of a renal sodium/dicarboxylate cotransporter. J. Biol. Chem. **270**, 5779–5785

4 Pajor, A. M. and Sun, N. (1996) Functional differences between rabbit and human Na^+-dicarboxylate cotransporters, NaDC-1 and hNaDC-1. Am. J. Physiol. **271**, F1093–F1099

5 Bai, L. and Pajor, A. M. (1997) Expression cloning of NaDC-2, an intestinal Na^+- or Li^+-dependent dicarboxylate transporter. Am. J. Physiol. **273**, G267–G274

6 Sekine, T., Cha, S. H., Hosoyamada, M., Kanai, Y., Watanabe, N., Furuta, Y., Fukuda, K., Igarashi, T. and Endou, H. (1998) Cloning, functional characterization, and localization of a rat renal Na^+-dicarboxylate transporter. Am. J. Physiol. **275**, F298–F305

7 Chen, X. Z., Shayakul, C., Berger, U. V., Tian, W. and Hediger, M. A. (1998) Characterization of a rat Na^+-dicarboxylate cotransporter. J. Biol. Chem. **273**, 20972–20981

8 Kekuda, R., Wang, H., Huang, W., Pajor, A. M., Leibach, F. H., Devoe, L. D., Prasad, P. D. and Ganapathy, V. (1999) Primary structure and functional characteristics of a mammalian sodium-coupled high affinity dicarboxylate transporter. J. Biol. Chem. **274**, 3422–3429

9 Chen, X., Tsukaguchi, H., Chen, X. Z., Berger, U. V. and Hediger, M. A. (1999) Molecular and functional analysis of SDCT2, a novel rat sodium-dependent dicarboxylate transporter. J. Clin. Invest. **103**, 1159–1168

10 Pajor, A. M. and Sun, N. N. (2000) Molecular cloning, chromosomal organization, and functional characterization of a sodium-dicarboxylate cotransporter from mouse kidney. Am. J. Physiol. Renal Physiol. **279**, F482–F490

11 Huang, W., Wang, H., Kekuda, R., Fei, Y. J., Friedrich, A., Wang, J., Conway, S. J., Cameron, R. S., Leibach, F. H. and Ganapathy, V. (2000) Transport of N-acetylaspartate by the Na^+-dependent high-affinity dicarboxylate transporter NaDC3 and its relevance to the expression of the transporter in the brain. J. Pharmacol. Exp. Ther. **295**, 392–403

12 Wang, H., Fei, Y. J., Kekuda, R., Yang-Feng, T. L., Devoe, L. D., Leibach, F. H., Prasad, P. D. and Ganapathy, V. (2000) Structure, function, and genomic organization of human Na^+-dependent high-affinity dicarboxylate transporter. Am. J. Physiol. Cell Physiol. **278**, C1019–C1030

13 Rogina, B., Reenan, R. A., Nilsen, S. P. and Helfand, S. L. (2000) Extended life-span conferred by cotransporter gene mutations in *Drosophila*. Science **290**, 2137–2140

14 Inoue, K., Fei, Y. J., Huang, W., Zhuang, L., Chen, Z. and Ganapathy, V. (2002) Functional identity of *Drosophila melanogaster* Indy as a cation-independent, electroneutral transporter for tricarboxylic acid-cycle intermediates. Biochem. J. **367**, 313–319

15 Knauf, F., Rogina, B., Jiang, Z., Aronson, P. S. and Helfand, S. L. (2002) Functional characterization and immunolocalization of the transporter encoded by the life-extending gene Indy. Proc. Natl. Acad. Sci. U.S.A. **99**, 14315–14319

16 Inoue, K., Zhuang, L., Maddox, D. M., Smith, S. B. and Ganapathy, V. (2002) Structure, function, and expression pattern of a novel sodium-coupled citrate transporter (NaCT) cloned from mammalian brain. J. Biol. Chem. **277**, 39469–39476

17 Inoue, K., Zhuang, L. and Ganapathy, V. (2002) Human Na^+-coupled citrate transporter: primary structure, genomic organization, and transport function. Biochem. Biophys. Res. Commun. **299**, 465–471

18 Inoue, K., Zhuang, L., Maddox, D. M., Smith, S. B. and Ganapathy, V. (2003) Human sodium-coupled citrate transporter, the orthologue of *Drosophila* Indy, as a novel target for lithium action. Biochem. J. **374**, 21–26

19 Sulston, J. and Hodgkin, J. (1988) Methods. In The Nematode *Caenorhabditis elegans* (Wood, W. B. and the community of *C. elegans* researchers, eds.), pp. 587–606, Cold Spring Harbor Press, Cold Spring Harbor, NY

20 Lewis, J. A. and Fleming, J. T. (1995) Basic culture methods. Methods Cell Biol. **48**, 3–29

21 Fei, Y. J., Fujita, T., Lapp, D. F., Ganapathy, V. and Leibach, F. H. (1998) Two oligopeptide transporters from *Caenorhabditis elegans*: molecular cloning and functional expression. Biochem. J. **332**, 565–572
22 Fei, Y. J., Romero, M. F., Krause, M., Liu, J. C., Huang, W., Ganapathy, V. and Leibach, F. H. (2000) A novel H^+-coupled oligopeptide transporter (OPT3) from *Caenorhabditis elegans* with a predominant function as a H^+ channel and an exclusive expression in neurons. J. Biol. Chem. **275**, 9563–9571
23 Fei, Y. J., Kanai, Y., Nussberger, S., Ganapathy, V., Leibach, F. H., Romero, M. F., Singh, S. K., Boron, W. F. and Hediger, M. A. (1994) Expression cloning of a mammalian proton-coupled oligopeptide transporter. Nature (London) **368**, 563–566
24 Mackenzie, B., Fei, Y. J., Ganapathy, V. and Leibach, F. H. (1996) The human intestinal H^+/oligopeptide cotransporter hPEPT1 transports differently-charged dipeptides with identical electrogenic properties. Biochim. Biophys. Acta **1284**, 125–128
25 Mello, C. and Fire, A. (1995) DNA transformation. Methods Cell Biol. **48**, 451–482
26 Kramer, J. M., French, R. P., Park, E. C. and Johnson, J. J. (1990) The *Caenorhabditis elegans rol*-6 gene, which interacts with the sqt-1 collagen gene to determine organismal morphology, encodes a collagen. Mol. Cell Biol. **10**, 2081–2089
27 Miller, D. M. and Shakes, D. C. (1995) Immunofluorescence microscopy. Methods Cell Biol. **48**, 365–394
28 Chalfie, M., Tu, Y., Euskirchen, G., Ward, W. W. and Prasher, D. C. (1994) Green fluorescent protein as a marker for gene expression. Science **263**, 802–805
29 Fire, A., Xu, S., Montgomery, M. K., Kostas, S. A., Driver, S. E. and Mello, C. C. (1998) Potent and specific genetic interference by double-stranded RNA in *Caenorhabditis elegans*. Nature (London) **391**, 806–811
30 Timmons, L., Court, D. L. and Fire, A. (2001) Ingestion of bacterially expressed dsRNAs can produce specific and potent genetic interference in *Caenorhabditis elegans*. Gene **263**, 103–112
31 McCulloch, D. and Gems, D. (2003) Body size, insulin/IGF signaling and aging in the nematode *Caenorhabditis elegans*. Exp. Gerontol. **38**, 129–136
32 Greenspan, P., Mayer, E. P. and Fowler, S. D. (1985) Nile red: a selective fluorescent stain for intracellular lipid droplets. J. Cell Biol. **100**, 965–973
33 Ashrafi, K., Chang, F. Y., Watts, J. L., Fraser, A. G., Kamath, R. S., Ahringer, J. and Ruvkun, G. (2003) Genome-wide RNAi analysis of *Caenorhabditis elegans* fat regulatory genes. Nature (London) **421**, 268–272
34 Kenyon, C., Chang, J., Gensch, E., Rudner, A. and Tabtiang, R. (1993) A *C. elegans* mutant that lives twice as long as wild type. Nature (London) **366**, 461–464
35 Wolkow, C. A., Kimura, K. D., Lee, M. S. and Ruvkun, G. (2000) Regulation of *C. elegans* life-span by insulinlike signaling in the nervous system. Science **290**, 147–150
36 Krebs, H. A. (1950) Chemical composition of blood plasma and serum. Annu. Rev. Biochem. **19**, 409–430
37 Nordmann, J. and Nordmann, R. (1961) Organic acids in blood and urine. Adv. Clin. Chem. **4**, 53–120

Received 25 November 2003; accepted 16 December 2003
Published as BJ Immediate Publication 16 December 2003, DOI 10.1042/BJ20031807